

## Softening and Broadening of the Zone Boundary Magnons in $\text{Pr}_{0.63}\text{Sr}_{0.37}\text{MnO}_3$

H. Y. Hwang,<sup>1</sup> P. Dai,<sup>2</sup> S-W. Cheong,<sup>1</sup> G. Aeppli,<sup>3</sup> D. A. Tennant,<sup>2</sup> and H. A. Mook<sup>2</sup>

<sup>1</sup>*Bell Laboratories, Lucent Technologies, Murray Hill, New Jersey 07974*

<sup>2</sup>*Solid State Division, Oak Ridge National Laboratory, Oak Ridge, Tennessee 37831*

<sup>3</sup>*NEC Research Institute, 4 Independence Way, Princeton, New Jersey 08540*

(Received 14 March 1997; revised manuscript received 3 October 1997)

We have studied the spin dynamics in  $\text{Pr}_{0.63}\text{Sr}_{0.37}\text{MnO}_3$  above and below the Curie temperature  $T_C = 301$  K. Three distinct new features have been observed: a softening of the magnon dispersion at the zone boundary for  $T < T_C$ , significant broadening of the zone boundary magnons as  $T \rightarrow T_C$ , and no evidence for residual spin-wave-like excitations just above  $T_C$ . The results are inconsistent with double exchange models that have been successfully applied to higher  $T_C$  samples, indicating an evolution of the spin system with decreasing  $T_C$ . [S0031-9007(97)05186-7]

PACS numbers: 75.30.Ds

The revival in the study of manganites has led to a reexamination of the unique coupling between magnetism and charge transport in these materials. We focus on perovskite manganites with a transition from a high temperature paramagnetic insulator to a low temperature ferromagnetic metal at the Curie temperature  $T_C$ . The samples that exhibit this behavior have been partially hole doped away from a parent antiferromagnetic insulator, such as  $\text{LaMnO}_3$ , by divalent substitution on the La site, such as  $\text{La}_{0.7}\text{Ca}_{0.3}\text{MnO}_3$  [1]. The Mn 3d levels, split by the oxygen octahedral crystal field to a lower energy  $t_{2g}$  triplet and a higher energy  $e_g$  doublet, are filled according to Hund's rule such that all spins are aligned on a given site by a large intra-atomic exchange  $J_H$ . Electronic conduction arises from the hopping of an electron from  $\text{Mn}^{3+}$  to  $\text{Mn}^{4+}$  with electron transfer energy  $t$ . This results in the ferromagnetic double exchange interaction between localized  $S = 3/2$  spins (the core  $t_{2g}$  triplet) mediated by the hopping  $e_g$  electron [2,3].

Recently, it has been shown that although the highest  $T_C$  materials are reasonably described by the double exchange model, with decreasing  $T_C$  (and reduced electronic bandwidth), the dramatic magnetotransport properties and increasingly first-order transition require the incorporation of a strong Jahn-Teller based phonon coupling [4–6]. This has been corroborated by a number of studies showing the growing importance of static and dynamic lattice distortions as the zero temperature insulating state is approached [7,8]. Thus far, most studies of the spin dynamics have focused on high  $T_C$  samples which have been shown to be consistent with the double exchange model [9–11]. With decreasing  $T_C$  however, important deviations may occur, as indicated by the development of a prominent diffusive central peak near  $T_C$  in  $\text{La}_{0.67}\text{Ca}_{0.33}\text{MnO}_3$  ( $T_C = 250$  K) [12]. By studying the spin dynamics in a sample with reduced  $T_C$ , we can test if the spin system remains well described by simple double exchange (allowing for renormalizations of  $t$  and  $J_H$ ), or just as for the charge dynamics, the lattice coupling must be explicitly considered.

In this paper we report a neutron scattering study of the magnetic dynamics in  $\text{Pr}_{0.63}\text{Sr}_{0.37}\text{MnO}_3$  above and below  $T_C = 301$  K, focusing on the zone boundary magnons. At 10 K ( $0.03T_C$ ), the magnons are well defined for all wave vectors  $q$  and exhibit a significant deviation from the dispersion associated with the simplest local moment description. At 265 K ( $0.9T_C$ ), the dispersion relation has uniformly softened but maintains its  $q$  dependence, and significant broadening of the short wavelength magnons is observed. At 315 K ( $1.05T_C$ ), just 14 K above  $T_C$ , there is no evidence for an inelastic magnetic peak at any  $q$ . We argue that these observations are at odds with double exchange calculations of the spin excitations (including leading order self-energy corrections), indicating qualitatively different spin dynamics in lower  $T_C$  samples.

We used the floating zone method to grow a large single crystal of  $\text{Pr}_{0.63}\text{Sr}_{0.37}\text{MnO}_3$  with a mosaic spread of  $0.5^\circ$  full-width at half maximum (FWHM). The neutron scattering measurements were carried out on the HB1 triple-axis spectrometer at the High-Flux Isotope Reactor, Oak Ridge National Laboratory. The collimations were, proceeding from the reactor to the detector,  $50'-40'-S-40'-70'$ , and the final neutron energy was fixed at  $E_f = 13.5$  or 30.5 meV. The monochromator, analyzers and filters were all pyrolytic graphite. The sample was slightly orthorhombic and twinned at the measured temperatures. Even so, we assumed a cubic lattice ( $a_0 = 3.86 \text{ \AA}$ ) because we could not resolve the effects of the twinning within the spectrometer resolution.

Figure 1 shows the magnon dispersion along the  $[0, 0, 1]$ ,  $[1, 1, 0]$ , and  $[1, 1, 1]$  directions at 10 K, and along  $[0, 0, 1]$  at 265 K ( $0.9T_C$ ). Figure 2 shows some of the constant  $q$  scans from which Fig. 1 was obtained. The experimentally observed magnon peaks were accurately described by Gaussian fits. To verify that our results are not instrumental artifacts, we performed a four-dimensional Monte Carlo convolution of the experimental resolution function [13] and the theoretical neutron scattering cross section for damped spin waves. We verified that the peak positions were relatively unchanged,

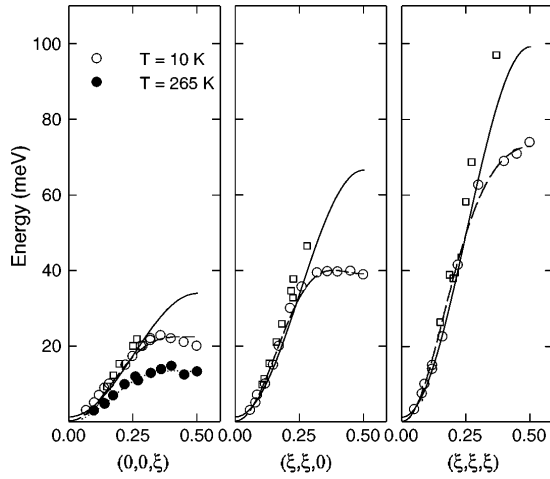


FIG. 1. Magnon dispersions for  $(0,0,\xi)$ ,  $(\xi,\xi,0)$ , and  $(\xi,\xi,\xi)$  (where  $\xi = 0.5$  is the cubic zone boundary) at  $T = 10$  and  $265$  K. The solid line is a fit to a nearest-neighbor Hamiltonian for  $T = 10$  K and  $\xi < 0.2$ . The dashed line is a fit for all data including up to fourth nearest neighbors at  $T = 10$  K. The dotted line is the corresponding four neighbor fit for  $T = 265$  K. Also shown in squares are data for  $\text{La}_{0.7}\text{Pb}_{0.3}\text{MnO}_3$  at  $10$  K (from Ref. [10]).

especially near the zone boundary saddle point, where significant resolution-induced shifts could occur. Our calculations place an upper bound of  $0.5$  meV for the shift in the peak position due to resolution effects. Another possible source of misinterpretation is that the broad peak at  $(0,0,1.4)$  at  $265$  K is actually a composite of phonon as well as magnon peaks. This was ruled out by measuring the same point in the next zone, which showed the same line shape, down in intensity by the magnetic form factor.

Focusing first on the low temperature dispersion, a new feature we have observed is the significant softening at the zone boundary, seen in all directions. The Heisenberg spin Hamiltonian,  $H = -\sum_{ij} J_{ij} \mathbf{S}_i \cdot \mathbf{S}_j$ , couples the spins at site  $R_i$  and  $R_j$  by  $J_{ij}$ . In the linear approximation, the spin wave dispersion relation is given by  $\hbar\omega(\mathbf{q}) = \Delta + 2S[J(\mathbf{0}) - J(\mathbf{q})]$ , where  $J(\mathbf{q}) = \sum_j J_{ij} \exp[i\mathbf{q} \cdot (R_i - R_j)]$ .  $\Delta$  allows for small anisotropies. The solid line in Fig. 1 is the outcome of a fit for only nearest-neighbor interactions for  $\xi < 0.2$  (the cubic zone boundary occurs at  $\xi = 0.5$ ), resulting in  $\Delta = 1.3 \pm 0.3$  meV and  $2SJ_1 = 8.2 \pm 0.5$  meV. Although this describes the data for  $\xi < 0.2$ , the zone boundary magnons are missed by  $15$ – $30$  meV. By comparison, the magnon dispersion in  $\text{La}_{0.7}\text{Pb}_{0.3}\text{MnO}_3$  ( $T_C = 355$  K) was found to be well described by only nearest-neighbor interactions of similar strength [10].

The dashed lines in Fig. 1 are a fit to the full data set including up to fourth neighbor interactions, resulting in  $\Delta = 0.2 \pm 0.3$  meV,  $2SJ_1 = 5.58 \pm 0.07$  meV,  $2SJ_2 = -0.36 \pm 0.04$  meV,  $2SJ_3 = 0.36 \pm 0.04$  meV, and  $2SJ_4 = 1.48 \pm 0.10$  meV. This accurately follows the dispersion except near the  $[0,0,1]$  zone boundary,

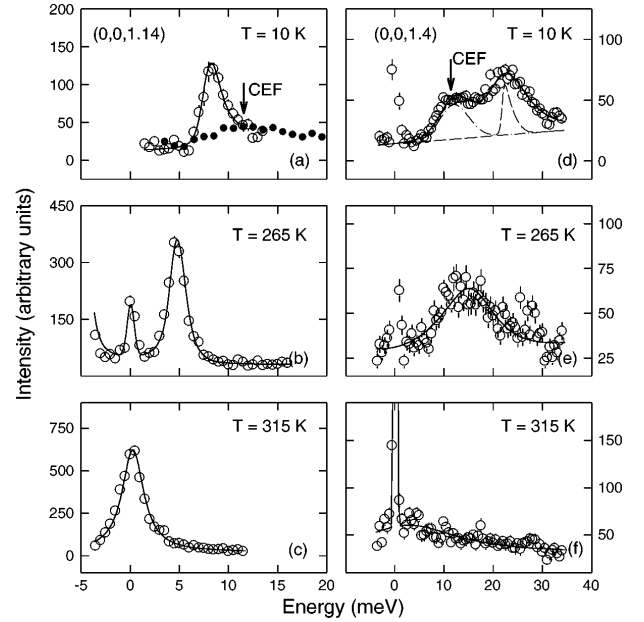


FIG. 2. Constant- $q$  scans at two different wave vectors with the left panel close to the zone center and the right panel close to the zone boundary. There is a dispersionless crystal electric field (CEF) level at  $\sim 12$  meV from Pr (shown as dash-dot line). The solid circles are a constant- $q$  scan of the CEF level at  $(0,0,1)$ , the zone center. At  $265$  K, the intensity of the CEF level drops to undetectable levels and has therefore been ignored in the data analysis at this temperature. The  $T = 315$  K data have been fitted with a simple Lorentzian line shape (including a Gaussian). The other data have been fitted to a damped harmonic oscillator, including 4D convolution of the instrumental resolution as described in the text. The dashed line is the instrumental response to spin waves with infinite lifetimes and the dispersion shown in Fig. 1.

which requires the next Fourier term in this direction, corresponding to  $J_8$ . Nevertheless, the fourth nearest-neighbor fit quantifies the remarkable result that *additional extremely long range ferromagnetic couplings are required*. Although  $J_2$  and  $J_3$  were necessary to fit the data, the more important correction to nearest-neighbor coupling is  $J_4$ . The long range and nonmonotonic behavior of  $J(\mathbf{q})$  required by the data seems to rule out a simple Heisenberg Hamiltonian.

On warming, the dispersion relation uniformly softens, as can be seen in Figs. 1 and 2 for the  $[0,0,1]$  branch at  $265$  K. At  $\xi = 0.14$ , near the zone center, the magnon peak shows no substantial changes other than decreasing to lower energy as temperature is increased. In addition, it is resolution limited at both  $10$  and  $265$  K. Just above  $T_C$ , at  $315$  K, there is no evidence for the magnon peak as expected for the long-wavelength excitations. As the Brillouin zone is traversed (Fig. 3), magnon lifetime effects become apparent. In particular, on approaching the zone boundary at  $\xi = 0.5$ , the  $10$  K linewidth is substantially larger than the experimental resolution width. On warming to  $265$  K, the deconvolved

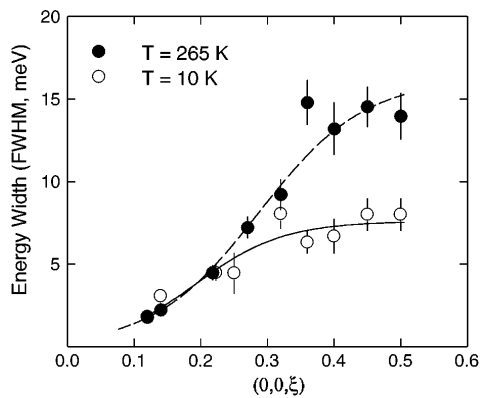


FIG. 3. Magnon line widths in the  $[0, 0, 1]$  direction extracted from Gaussian fits with a sloping background. The solid and dashed lines are guides to the eye.

widths, which we quote as full widths at half maximum throughout this paper and its figures, are nearly doubled, from their 10 K value of  $8.4 \pm 0.5$  meV to  $13.2 \pm 1.9$  meV. Again, at  $315$  K  $> T_C$ , no obvious magnon peak remains.

An important issue to address is the role of the magnetic Pr ions, which display the crystal electric field (CEF) level shown in Fig. 2. A recent powder neutron diffraction study of a manganite with similar Pr concentration observed a refined ferromagnetic moment of  $\sim 0.5\mu_B$  at low temperature [14]. Thus the proper description of the total spin system involves a two component non-Bravais lattice. A bound on possible Pr-Mn interactions can be placed by examining the crossing of the CEF level and the magnon dispersion, for example near  $\xi = 0.2$  in the  $[0, 0, 1]$  branch. Even for weak coupling, this region is susceptible to the effects of mixing due to energy degeneracy. Experimentally, we find that the CEF level varies smoothly through the crossing of the magnon branch without dispersion. The integrated intensities of both the CEF excitation and the magnons show no anomaly at their crossing, and in particular, the observed magnon linewidth presented in Fig. 3 shows no feature at the crossing. Also, the magnon dispersion passes smoothly through the CEF level just as in  $\text{La}_{0.7}\text{Pb}_{0.3}\text{MnO}_3$ , which does not contain a magnetic rare earth ion (Fig. 1). Thus, our experiments show no evidence for Mn-Pr coupling with an effect on the Mn spin dynamics.

To place our study of  $\text{Pr}_{0.63}\text{Sr}_{0.37}\text{MnO}_3$  in proper context, it is useful to compare with more conventional ferromagnets. Perhaps the most relevant comparison is to the europium chalcogenides, insulating ferromagnets that are considered ideal Heisenberg spin systems with extended exchange interactions (next nearest-neighbor interactions are significant) [15–17]. In EuO, both  $J_1$  and  $J_2$  are ferromagnetic, whereas in EuS,  $J_2$  is a competing anti-ferromagnetic interaction with  $J_1$  (higher order terms are negligible). Although similar to  $\text{Pr}_{0.63}\text{Sr}_{0.37}\text{MnO}_3$  in this respect, the abrupt zone boundary softening we have ob-

served (not seen in the europium chalcogenides) requires a large  $J_4$ , while  $J_2$  and  $J_3$  are relatively small. Despite the large difference in  $T_C$  for EuO ( $T_C = 69.2$  K) and EuS ( $T_C = 16.6$  K), the low frequency spin stiffness, magnon bandwidth, and  $T_C$  are self-consistently related via simple mean field theory. Comparison of the two manganite samples with  $T_C = 355$  K and  $T_C = 301$  K (Fig. 1) shows that at low energy, the magnon dispersions are almost identical, while the zone boundary softening of the lower  $T_C$  sample results in a  $\sim 31\%$  decrease in the magnon bandwidth from  $\sim 108$  meV to  $\sim 74$  meV. Although  $\text{La}_{0.7}\text{Pb}_{0.3}\text{MnO}_3$  is roughly consistent with mean field theory, with decreasing  $T_C$  this breaks down because the spin stiffness does not diminish—the additional exchange constants have been exactly balanced by a reduction in the effective  $J_1$  to give the same low frequency spin stiffness.

The spin dynamics of both EuO and EuS have been extensively studied [18,19], and the damping near  $T_C$  in both cases was observed to vary consistent with predominant magnon-magnon damping [20,21], with the linewidth  $\Gamma$  varying as  $\Gamma \propto q^4 \ln^2(k_B T / \hbar \omega_{\mathbf{q}})$  for  $\hbar \omega_{\mathbf{q}} \ll k_B T$ , and  $\Gamma \propto q^3$  for  $\hbar \omega_{\mathbf{q}} \gg k_B T$ . Although theoretically valid only in limiting extremes, and for  $(a_0 q)^2 \ll 1$ ,  $\Gamma(q)$  was observed to rise smoothly across  $\hbar \omega_{\mathbf{q}} = k_B T$  in EuS. By contrast, we have observed the lack of a  $q$  dependence near the zone boundary for  $\xi > 0.35$ . At present, it remains unclear whether our results indicate another important damping channel (quasiparticles, lattice distortions), or whether a revised spin wave theory which takes account of the unusual spin wave dispersion for  $\text{Pr}_{0.63}\text{Sr}_{0.37}\text{MnO}_3$  is sufficient. Finally, in both EuO and EuS, at short wavelengths, a magnonlike peak was observed far above  $T_C$ , whereas we did not observe such a feature just above  $T_C$  in  $\text{Pr}_{0.63}\text{Sr}_{0.37}\text{MnO}_3$  for any  $\xi$  in the  $[0, 0, 1]$  branch.

We now discuss possible explanations of our results. Within a Stoner model, the conduction band in the ferromagnetic state is exchange split into a majority and minority band. The magnon dispersion enters the Stoner continuum at finite  $q$  and  $\omega$ , where quasiparticle damping of spin waves occurs. The ferromagnetic ground state of the manganite, however, is rather unique in that there is complete separation of the majority and minority band by a large  $J_H$ . Thus at low temperatures, the entire spin wave dispersion probably lies below the triplet electron-hole pair excitation continuum. At temperatures approaching  $T_C$ , however, the ordered moment is decreased and the carriers are no longer fully polarized, bringing triplet electron-hole pair excitations to energies within the spin wave band. These excitations can be the decay products of low energy magnons, and as their probability rises with temperature, result in temperature-dependent magnon lifetimes.

The damping mechanism described above can be encapsulated in the imaginary part of the magnon self energy. The real part contains the magnon dispersion,

including its deviations from a simple cosine form. The magnon dispersion incorporating the lowest order self-energy correction has been calculated in a Kondo lattice model Hamiltonian with ferromagnetic spin-electron exchange [11]. For  $J_H/t = \infty$ , the result was a simple cosine dispersion consistent with a nearest-neighbor ferromagnetic Heisenberg exchange. For finite values of  $J_H/t$ , there are deviations from the simple result, but the deviations do not fit our experimental observations. In particular, the reduction of the low frequency spin stiffness is more significant than the reduction of the total bandwidth, contrary to the experimental results emphasized earlier. Beyond these inconsistencies, however, the most important point is that with decreasing  $T_C$ ,  $t$  is reduced.  $J_H$  is presumably unchanged, being an intraatomic energy. Thus with decreasing  $T_C$ , corrections of order  $t/J_H$  should decrease, not increase. Therefore, lowest order perturbative corrections in  $t/J_H$  do not capture our experimental results.

The Kondo-lattice calculations discussed above have two limitations: the rate of convergence is not well understood, and the effects of varying the hole concentration  $x$  are not explored. These issues have been studied in one dimension by exact diagonalization of double exchange coupled spin rings for large  $J_H$  [22,23]. Deviations from a simple cosine dispersion are predicted, particularly for extremely large or small doping ( $x < 0.2$  and  $x > 0.7$ ). For intermediate carrier concentrations (as studied here), however, a cosine band is recovered. For the two samples compared in Fig. 1, the nominal carrier concentration is not significantly different, leading to the conclusion that a degree of freedom beyond  $x$ ,  $t$ , or  $J_H$  is needed to account for our data.

One much discussed parameter beyond the purely electronic parameters is the electron-lattice coupling, which is worth considering because of the large and strongly temperature-dependent mean square displacements  $\langle \mathbf{u}^2 \rangle$  of Mn and O near  $T_C$  [7,8]. The bare overlap integral between the Mn spins is highly sensitive to the geometric arrangement of the Mn-O-Mn linkage, particularly due to the directional nature of the Mn  $d$  and O  $p$  orbitals. The softening of the well-defined zone boundary magnons at low temperature would then be due to slow (on the scale of the zone boundary spin wave energies) fluctuations towards doubling of the nuclear unit cell. That fluctuations of this type might exist is clear from the myriad of lattice and charge-ordering instabilities in the phase diagrams of the manganites. Coupling to the lattice can also contribute to the magnon lifetime effects in the manganites. In particular, the rapid rise in  $\langle \mathbf{u}^2 \rangle$  with temperature could give rise to a broadening distribution of effective exchange constants, leading to the pronounced broadening of the short wavelength magnons near  $T_C$ . Long wavelength magnons, of course, would not be affected as the variations in  $J$  would be averaged out. This scenario is qualitatively consistent with the  $T_C$  depen-

dence of the spin dynamics, in that the highest  $T_C$  samples do not show the strong feature in  $\langle \mathbf{u}^2 \rangle$  [9].

We thank B. Batlogg, J.A. Fernandez-Baca, N. Furukawa, Y.B. Kim, P.B. Littlewood, P. Majumdar, A. Millis, B.I. Shraiman, S.H. Simon, and C.M. Varma for useful discussions. H.Y.H. and G.A. would like to thank the HFIR staff at ORNL for their hospitality and assistance. The work at ORNL was supported by the U.S. DOE under Contract No. DE-AC05-96OR22464 with Lockheed Martin Energy Research, Inc.

- 
- [1] G.H. Jonker and J.H. Van Santen, *Physica (Utrecht)* **16**, 337 (1950).
  - [2] C. Zener, *Phys. Rev.* **82**, 403 (1951).
  - [3] P.W. Anderson and H. Hasegawa, *Phys. Rev.* **100**, 675 (1955).
  - [4] H.Y. Hwang, S-W. Cheong, P.G. Radaelli, M. Marezio, and B. Batlogg, *Phys. Rev. Lett.* **75**, 914 (1995).
  - [5] H. Röder, J. Zang, and A.R. Bishop, *Phys. Rev. Lett.* **76**, 1356 (1996).
  - [6] A.J. Millis, B.I. Shraiman, and R. Mueller, *Phys. Rev. Lett.* **77**, 175 (1996).
  - [7] P. Dai, J. Zhang, H.A. Mook, S.-H. Liou, P.A. Dowben, and E.W. Plummer, *Phys. Rev. B* **54**, 3694 (1996).
  - [8] P.G. Radaelli, M. Marezio, H.Y. Hwang, S-W. Cheong, and B. Batlogg, *Phys. Rev. B* **54**, 8992 (1996).
  - [9] M.C. Martin, G. Shirane, Y. Endoh, K. Hirota, Y. Moritomo, and Y. Tokura, *Phys. Rev. B* **53**, 14285 (1996).
  - [10] T.G. Perring, G. Aeppli, S.M. Hayden, S.A. Carter, J.P. Remeika, and S-W. Cheong, *Phys. Rev. Lett.* **77**, 711 (1996).
  - [11] N. Furukawa, *J. Phys. Soc. Jpn.* **65**, 1174 (1996).
  - [12] J.W. Lynn, R.W. Erwin, J.A. Borchers, Q. Huang, A. Santoro, J-L. Peng, and Z.Y. Li, *Phys. Rev. Lett.* **76**, 4046 (1996).
  - [13] M.J. Cooper and R. Nathans, *Acta Crystallogr.* **23**, 357 (1967).
  - [14] P.G. Radaelli, G. Iannone, D.E. Cox, M. Marezio, H.Y. Hwang, and S-W. Cheong, *Physica (Amsterdam) B* (to be published).
  - [15] L. Passell, O.W. Dietrich, and J. Als-Nielsen, *Phys. Rev. B* **14**, 4897 (1976).
  - [16] H.G. Bohn, W. Zinn, B. Dorner, and A. Kollmar, *Phys. Rev. B* **22**, 5447 (1980).
  - [17] H.A. Mook, *Phys. Rev. Lett.* **46**, 508 (1981).
  - [18] O.W. Dietrich, J. Als-Nielsen, and L. Passell, *Phys. Rev. B* **14**, 4923 (1976).
  - [19] H.G. Bohn, A. Kollmar, and W. Zinn, *Phys. Rev. B* **30**, 6504 (1984).
  - [20] V.G. Vaks, A.I. Larkin, and S.A. Pikin, *Sov. Phys. JETP* **26**, 647 (1968).
  - [21] A.B. Harris, *Phys. Rev.* **175**, 674 (1968).
  - [22] J. Zang, H. Röder, A.R. Bishop, and S.A. Trugman, *J. Phys. Condens. Matter* (to be published).
  - [23] T.A. Kaplan and S.D. Mahanti, *J. Phys. Condens. Matter* (to be published).